ChemComm

COMMUNICATION

View Article Online
View Journal | View Issue

Cite this: *Chem. Commun.*, 2023, **59**, 1951

Received 28th November 2022,
Accepted 19th January 2023

DOI: 10.1039/d2cc06461h

rsc.li/chemcomm

Double click macrocyclization with Sondheimer diyne of aza-dipyrrins for B–F_{ree} bioorthogonal imaging†

Dan Wu, Gonzalo Durán-Sampedro, Sheila Fitzgerald, Massimiliano Garre and Donal F. O'Shea *

Sequential azide/diyne cycloadditions proved highly effective for the macrocyclization of a bis-azido aza-dipyrrin. Macrocyclic aza-dipyrrin could be produced in 30 min at rt in water with changes in fluorescence intensity and lifetimes measurable upon reaction. Live cell microscopy showed that aza-dipyrrins were suitable for confocal and STED super-resolution imaging and a bioorthogonal response to macrocyclization could be detected in cellular compartments. These results will encourage a broader examination of the sensing and imaging uses of aza-dipyrrins.

Dipyrrins and aza-dipyrrins (pyrrole bridging atom being N instead of C) are an often overlooked intermediate along the synthetic pathway to their metalloid (*e.g.* boron) or metal (*e.g.* Zn, Ag, Cu, Ni, Au, Ag) chelates.[1] The BF_2 chelates of (aza)-dipyrrins are by far the most popular and widely exploited for sensing and imaging applications as they are highly emissive.[2] In contrast, their dipyrrin or aza-dipyrrin precursors are reported to be either entirely non-emissive or very weakly emissive.[3,4] Arguably, this feature has caused them to be essentially unexploited for sensing and imaging applications. In this communication, we highlight the synthesis of a macrocyclic constrained fluorescent aza-dipyrrin with the ring closing reaction achievable under bioorthogonal conditions with a fluorogenic response permitting its monitoring in live cells.

As macrocyclization reactions are often low yielding, suffering from unwanted oligomerizations, a unique double strain promoted azide cycloaddition ring closure using Sondheimer diyne **1** was developed (Fig. 1).[5] The sequential cycloaddition of **1** with two equivalence of azide is known to produce the saddle shaped dibenzo-cycloocta-bis-1,2,3-triazoles **2** without the requirement of a catalyst.[5b] These reactions have been successfully employed for bio-conjugation, labelling and crosslinking of peptides, carbohydrates and oligo nucleotides.[6]

In this work we were interested to exploit this double click sequence for macrocyclization reactions with aza-dipyrrins of general structure **3** (Fig. 1, structures with blue lines). We were attracted to this approach as experimentally it has been shown that in the reaction of **1** with butyl azide the second cycloaddition is more than 500-fold faster than the first.[6f] This can be accounted for by the increase in acetylenic strain in the intermediate mono-triazolo adduct of **1** following the first cycloaddition. If this held true for a bis azide substrate then the ring closing second cycloaddition could be orders of magnitude faster than the first, thereby favouring it over oligomerization.

The synthesis of our targeted bis-azido substituted compound **7** commenced from the previously reported tetrahydropyran (THP) protected 6-hydroxy-1-(4-methoxyphenyl)-3-(nitromethyl) hexane-1-one **4** which was deprotected under acidic conditions yielding the alcohol **5** (Scheme 1).[7] Compound **5** was converted to its corresponding mesylate (Ms) by reaction with methanesulfonyl chloride, following which nucleophilic substitution with sodium azide introduced the azido-functional group into **6** in a high 85% yield. Subsequent treatment of **6** with NH_4OAc in

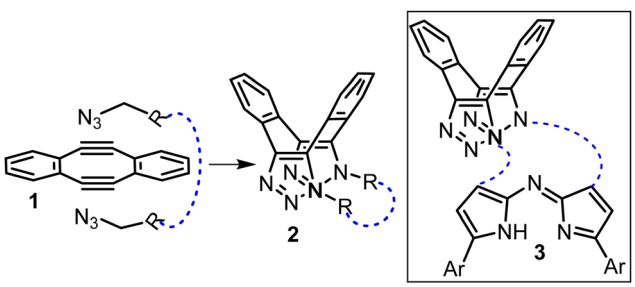

Fig. 1 Double azide cycloadditions with diyne **1** and its potential for macrocyclization to **2** (blue dashed line). Inset: Generic target structure of aza-dipyrrin macrocycle **3** capped by dibenzo-cycloocta-bis-1,2,3-triazole. Only *cis* isomers shown for clarity.

Department of Chemistry, RCSI, 123 St Stephen's Green, Dublin 2, Ireland. E-mail: donalfoshea@rcsi.ie

† Electronic supplementary information (ESI) available: Synthetic procedures, microscopy images, analytical data and spectra. See DOI: https://doi.org/10.1039/d2cc06461h

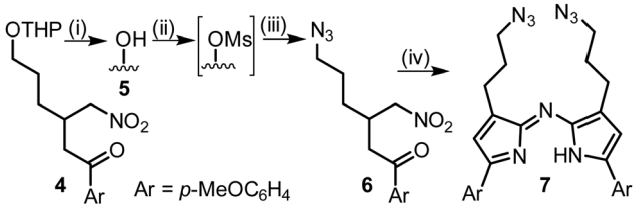

Scheme 1 Synthesis of bis-azide aza-dipyrrin **7**. Reaction conditions (i) *p*-TsOH, EtOH, reflux, 4 h, 91%. (ii) MsCl, TEA, DCM, 0 °C, 30 min. (iii) NaN_3, DMF, 4 h, reflux, 85%. (iv) NH_4OAc, MeOH, 9 h, reflux, 18%.

methanol under reflux for 9 h gave the targeted bis-azide substituted aza-dipyrrin 7 following purification by silica gel chromatography.

Next, a range of conditions were investigated for the double-click reaction of 7 with diyne **1** (Table 1). Encouragingly, in $CHCl_3$ at 8.6 mM concentration, it was found that the rt macrocyclization was a remarkably robust reaction, reaching completion in 3 h in overall 95% yield. No oligomeric products were observed which is consistent with the second intramolecular ring closing cycloaddition reaction being faster than the first. As is the case with other double azide cycloadditions with **1**, *cis* and *trans* isomers were obtained which are distinguishable by the relative positioning of the $N-1$ substituents from the triazole rings (Table 1, structures). Encouragingly, the favoured isomer, in a ratio of 2.6 : 1 was the *cis* product **8** which could be readily separated from the minor *trans* product **9** by silica chromatography (Table 1, entry 1).

Reaction times were relatively unaffected by choice of organic solvent with the rt reaction in MeOH (4 mM) reaching completion in 3 h, with the *cis*-**8**/*trans*-**9** isomeric ratios of 3.4 : 1 further favouring the *cis* product (entry 2, ESI,† Fig. S1). ^{1}H and ^{13}C NMR and HRMS analysis was consistent with the macrocyclic structures *cis*-**8** and *trans*-**9** (Fig. 2 and ESI,† Fig. S5, S6). ^{1}H NMR of **8** showed the two aryl rings of the dibenzocycloocta-bis-triazole saddle were non-equivalent with each having two CH resonances appearing as dd (ring (i) δ 7.60, 7.42 ppm, ring (ii) δ 7.13, 7.02 ppm) whereas the two *p*-methoxy aryl rings of the aza-dipyrrin were equivalent with two resonances integrating for four protons (δ 7.83, 7.08 ppm) (Fig. 2A and B). ^{1}H–^{1}H correlation spectroscopy (COSY) analysis of **8** showed the connectivity of the diastereotopic methylene protons bridging the aza-dipyrrin unit to the triazole rings (ESI,† Fig. S5). Nuclear Overhauser effect spectroscopy (NOESY) showed through-space interactions between the bridging macrocyclic N–CH methylene protons to aromatic ring (ii) of the saddle and between the β-pyrrole C–H and its methylene substituent (Fig. 2A structure, double headed arrows). Additionally, NOEs were observed between the pyrrole C–H and the neighbouring protons on the *p*-methoxy aryl ring. The distinguishing structural feature of *trans*-**9** was that the aryl rings of

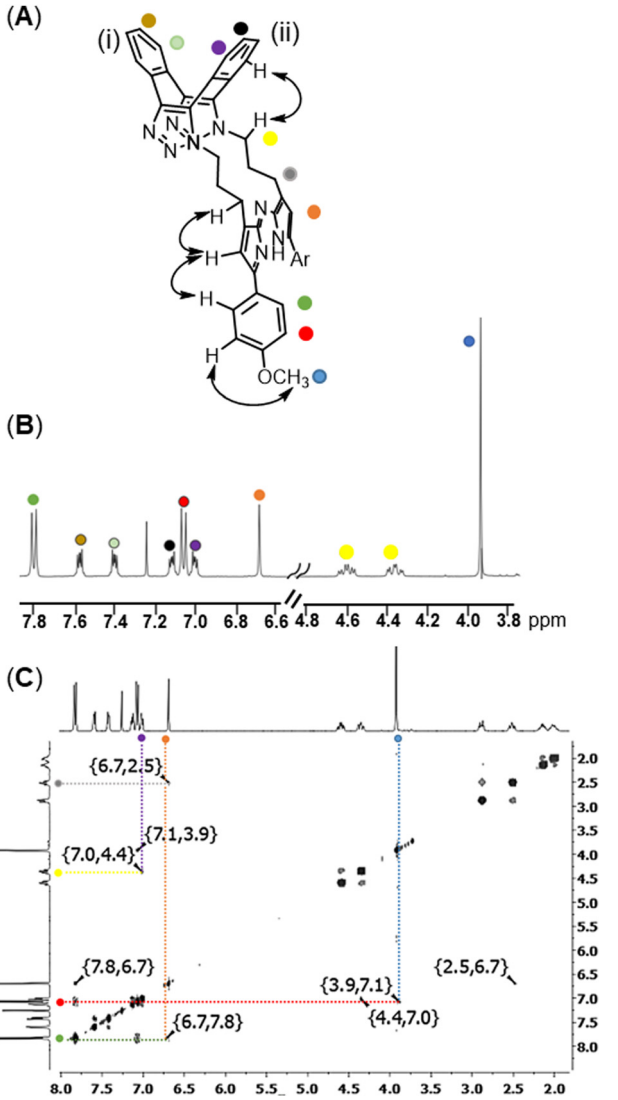

Fig. 2 (A) NMR characterization ($CDCl_3$ 400 MHz) of *cis*-**8** with double headed arrows showing key NOEs and coloured dots marking specific protons. (B) Partial ^{1}H NMR spectrum with coloured dots marking corresponding spectral peaks. (C) NOESY spectrum showing NOE correlations.

Table 1 Macrocyclization to *cis*-**8** and *trans*-**9** *via* double cycloaddition of **1** with **7**

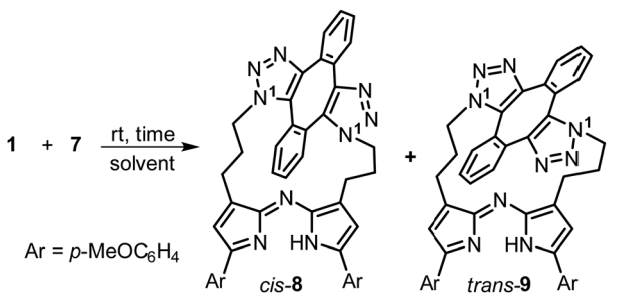

Entry	Solvent	Conc.	Time (h)	**8** : **9**[a]	**8**/**9** yield[b] (%)
1	$CHCl_3$	8.6 mM	3	2.6 : 1	69/26
2	MeOH	4 mM	3	3.4 : 1	73/22
3	MeOH	5 μM	5	3.3 : 1	73/22
4	H_2O[c]	5 μM	0.5	5.9 : 1	82/14

[a] Determined by ^{1}H NMR or HPLC. [b] Following separation by column chromatography. [c] With 0.3 mM polysorbate 20.

the saddle are equivalent which was observable in the COSY spectrum (ESI,† Fig. S6).

Next, the challenge was undertaken to identify macrocyclization conditions suitable for bioorthogonal live cell settings, which are restricted to micromolar range concentrations and 37 °C.[8] With this aim in mind, the reaction of **1** and **7** in water at a low concentration was tested, with reaction monitoring by HPLC and fluorescence spectroscopy. The acceleration of cycloaddition reactions in water is a known phenomenon which we sought to exploit using the surfactant polysorbate 20 (PS20) to assist in solubilizing the reagents.[9] PS20 is a fatty acid ester of polyethylene glycol substituted sorbitan with a critical micelle concentration (CMC) of 0.08 mM and is commonly used in the biotechnology industry.[10] Remarkably, the rt reaction of **7** and **1** (0.5 equiv.) in water containing 0.3 mM PS20 was highly efficient, reaching completion within 30 min in an overall 96% yield (Table 1, entry 4). As comparison under identical reaction concentrations in MeOH a reaction time of 5 h was required (entry 3, ESI,† Fig. S1). This extraordinary rate acceleration could be attributed to higher local substrate concentration as reagents are co-compartmentalised within lipophilic micelle nanoreactors of PS20, though water itself could also be a contributing factor.[9b] Also beneficially, the *cis* isomer **8** was increasingly favoured with a **8**/**9** ratio of 5.9 : 1 obtained (Table 1, entry 4). Absorption and emission spectra of **7** and **8** were recorded in water/PS20 as shown in Table 2A and B. For macrocyclic **8** absorbance and fluorescence λ_{max} were at 592 and 637 nm respectively with a quantum yield of 2.4% showing potential for use with microscopy imaging (Table 2, entry 2).

Monitoring the aqueous reaction progress by fluorescence spectroscopy showed that the emission at 637 nm increased 2.5 fold as the transformation of **7** into **8** proceeded (Table 2C and D). Phase lifetimes (τ_p) of **7** and **8** measured in water/PS20 showed significant differences at 0.25 and 0.7 ns respectively (Table 2, panel E, see ESI,† Fig. S10 and S11 for individual lifetimes).[11] Importantly, these distinguishable differences offer the potential for sensing the macrocyclization in live cells using fluorescence lifetime imaging microscopy (FLIM). A detectable change in photophysical properties in response to bioorthogonal transformations is an incredibly useful feature when imaging.[8] A limited number of fluorogenic azide cycloadditions have been reported in which the fluorescence intensity increases as a consequence of the azide group being transformed into a triazole.[12]

As neither dipyrrin nor aza-dipyrrin compounds have been previously utilized for fluorescence microscopy a live cell study of **7** and **8** was undertaken using confocal laser scanning microscopy (CLSM), stimulated emission depletion microscopy (STED) and FLIM. Incubation of MDA-MB 231 breast cancer cells with 5 μM solutions of either **7** or **8** for 1 h and CLSM imaging showed an effective internalization of both. Intracellular localization was noted in two regions, lipid droplets (LD) and secretory vacuoles (SV) for both aza-dipyrrins, though **8** was notably brighter than **7** (Fig. 3, panels A, ESI,† Fig. S12 and S13).[13]

The requirement of new fluorophore classes for the super resolution technique STED has been documented.[14] Pleasingly,

Table 2 Photophysical characteristics of aza-dipyrrins **7** and **8** and fluorogenic macrocyclization reaction in water/PS20[a]

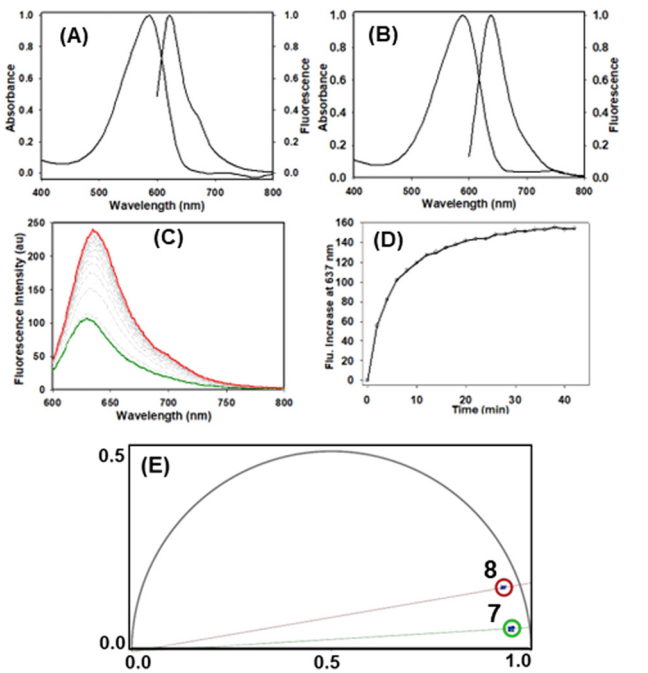

Entry	Comp.	Abs (nm)	Flu (nm)	Φ_{flu}[b] (%)	τ_p[c] (ns)
1	**7**	593	629	0.4	0.25
2	**8**	592	637	2.4	0.70

[a] Absorbance, fluorescence spectra recorded at 3 μM. [b] Nile red as standard. [c] Phase lifetime, see ESI for lifetime components.(A) Absorbance and emission spectra of **7**. (B) Absorbance and emission spectra of **8**. (C) Fluorogenic response (excit. 595 nm, 5 nm slit widths) during the reaction of **7** (5 μM) with **1** (5 μM) to produce **8**. (D) Plot of emission intensity at 637 nm from the reaction of **7** with **1** to produce **8**. (E) Overlaid phasor analysis of **7** (green circle, phase lifetime 0.25 ns) and **8** (red circle, phase lifetime 0.7 ns) (see ESI for **9** data).

8 was compatible with STED imaging giving the expected improved resolution, allowing the two subcellular compartments to be more clearly defined (Fig. 3 panels B and C, ESI,† Fig. S14). FLIM offers a distinct advantage for bioorthogonal imaging as the excited-state lifetimes of multiple fluorophores within different cellular compartments can be acquired simultaneously.[15] The phasor analysis of FLIM images allows a straightforward interpretation of these fluorescence signals and we sought to apply this to observe the intracellular reaction of **7** and **1**.[11,15] Phasor transformation of live cell FLIM images following incubation with **7** showed the phase lifetime of 0.4 ns (Fig. 4, panels A, B and see ESI,† Fig. S15 for FLIM images). We were delighted to observed that cells first treated with **7** to which **1** was subsequently added for 1 h showed a change in intracellular phase lifetime to 1.1 ns and matched that of cells treated with **8** alone (panel C, D see ESI,† Fig. S16 and S17 for FLIM images). As control, cells treated first with **8** for 1 h and then with **1** showed no change to the phasor plot (ESI,† Fig. S18). To the best of our knowledge, this is the first example of intracellular aza-dipyrrin spectral fluorescence, lifetime or bioorthogonal imaging.

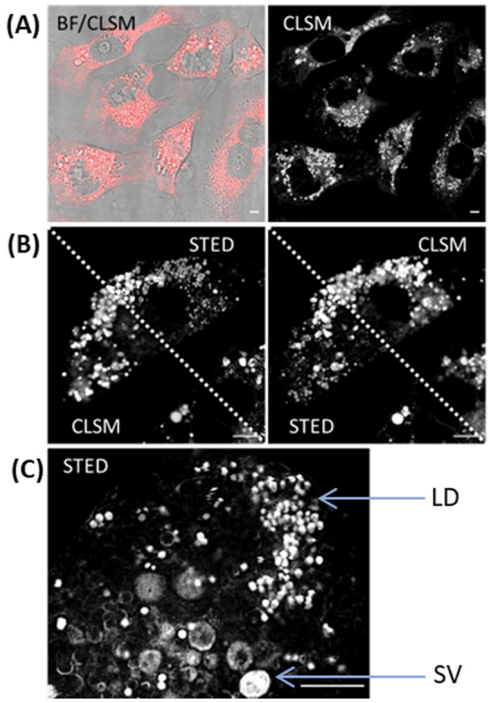

Fig. 3 Fluorescence microscopy imaging of MDA-MB 231 cells following 1 h incubation with *cis*-**8**, scale bars 5 μm. (A) CLSM image (fluorescence in red) with bright field (BF) overlay (left) and fluorescence shown in black and white for clarity (right). (B) Single cell imaged by both CLSM and STED with images split diagonally between both. (C) Expanded STED image showing lipid droplets (LD) and secretory vacuoles (SV) (see ESI,† Fig. S14 for replicate experiments and Fig. S12 for CLSM images of **7**).

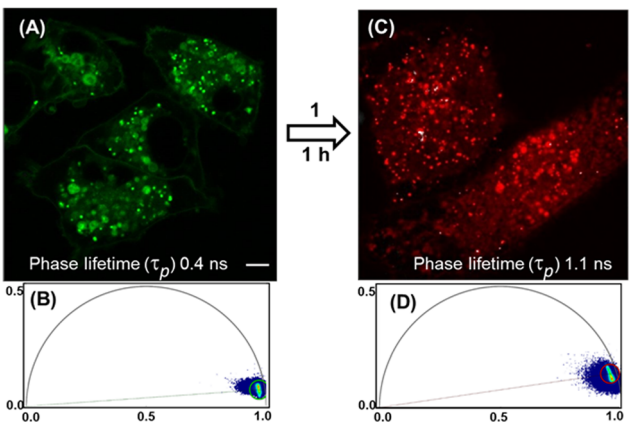

Fig. 4 Phasor analysed FLIM imaging of biorthogonal macrocyclization reaction of **7** (5 μM) with **1** (10 μM) in live MDA-MB 231 cells, scale bars 5 μm. (A) Phasor mapped FLIM image showing cells following 1 h incubation with **7**. (B) Phasor plot of intracellular **7**, green circle phase lifetime 0.4 ns. (C) Phasor mapped FLIM image showing cells pre-treated with **7** for 1 h followed by treatment with **1** for 1 h resulting in the transformation into **8**. (D) Phasor plot of intracellular **8** formed *via* bioorthogonal macrocyclization reaction (red circle, phase lifetime 1.1 ns).

In conclusion, the synthesis of a fluorescent macrocyclic aza-dipyrrin was achieved by a double 1,3-dipolar cycloaddition reaction in rt water or in live cells at 37 °C. Fluorogenic response to macrocyclization could be detected in different live cellular compartments using FLIM imaging. Further development of the B–F_{ree} aza-dipyrrins and their bioorthogonal applications is ongoing. Once unconstrained from their chelates, their overlooked value is revealed which may encourage a broader examination of their potential uses.

Financial support from Synthesis and Solid State Pharmaceutical Centre (SSPC) and Science Foundation Ireland (12/RC/2275) and EU Horizon 2020 Marie-Sklodowska-Curie grant agreement no. 707618. Images acquired in the RCSI Super Resolution Imaging Consortium funded by Science Foundation Ireland (18/RI/5723).

Conflicts of interest

There are no conflicts to declare.

Notes and references

1 (*a*) S. A. Baudron, *Dalton Trans.*, 2020, **49**, 6161; (*b*) R. Matsuoka and T. Nabeshima, *Front. Chem.*, 2018, **6**, 349; (*c*) R. S. Singh, R. P. Paitandi, R. K. Gupta and D. S. Pandey, *Coord. Chem. Rev.*, 2020, **414**, 213269; (*d*) A. Palma, J. F. Gallagher, H. Muller-Bunz, J. Wolowska, E. J. McInnes and D. F. O'Shea, *Dalton Trans.*, 2009, 273.
2 (*a*) Z. Shi, X. Han, W. Hu, H. Bai, B. Peng, L. Ji, Q. Fan, L. Li and W. Huang, *Chem. Soc. Rev.*, 2020, **49**, 7533; (*b*) H. Lu and Z. Shen, *Front. Chem.*, 2020, **8**, 290.
3 For useful discussion see; R. Liu, P. Vairaprakash and J. S. Lindsey, *New J. Chem.*, 2019, **43**, 9711.
4 M. Buyuktemiz, S. Duman and Y. Dede, *J. Phys. Chem. A*, 2013, **117**, 1665.
5 (*a*) H. N. C. Wong, P. J. Garratt and F. Sondheimer, *J. Am. Chem. Soc.*, 1974, **96**, 5604; (*b*) I. Kii, A. Shiraishi, T. Hiramatsu, T. Matsushita, H. Uekusa, S. Yoshida, M. Yamamoto, A. Kudo, M. Hagiwara and T. Hosoya, *Org. Biomol. Chem.*, 2010, **8**, 4051.
6 (*a*) K. Yao, A. Bertran, A. Howarth, J. M. Goicoechea, S. M. Hare, N. H. Rees, M. Foroozandeh, A. M. Bowen and N. J. Farrer, *Chem. Commun.*, 2019, **55**, 11287; (*b*) M. Tera and N. W. Luedtke, *Bioconjugate Chem.*, 2019, **30**, 2991; (*c*) H. Chen and Q. Miao, *ChemPlusChem*, 2019, **84**, 627; (*d*) S. Yoshida, J. Tanaka, Y. Nishiyama, Y. Hazama, T. Matsushita and T. Hosoya, *Chem. Commun.*, 2018, **54**, 13499; (*e*) Suguru Yoshida, Sayuri Goto, Yoshitake Nishiyama, Yuki Hazama, Masakazu Kondo, Takeshi Matsushita and Takamitsu Hosoya, *Chem. Lett.*, 2019, **48**, 1038; (*f*) D. A. Sutton and V. V. Popik, *J. Org. Chem.*, 2016, **81**, 8850; (*g*) S. Yoshida, A. Shiraishi, K. Kanno, T. Matsushita, K. Johmoto, H. Uekusa and T. Hosoya, *Sci. Rep.*, 2011, **1**, 82.
7 D. Wu, G. Durán-Sampedro and D. F. O'Shea, *Front. Chem. Sci. Eng.*, 2020, **14**, 97.
8 S. L. Scinto, D. A. Bilodeau, R. Hincapie, W. Lee, S. S. Nguyen, M. Xu, C. W. am Ende, M. G. Finn, K. Lang, Q. Lin, J. Paul Pezacki, J. A. Prescher, M. S. Robillard and J. M. Fox, *Nat. Rev. Methods Primers*, 2021, **1**, 30.
9 (*a*) M. Cortes-Clerget, J. Yu, J. R. A. Kincaid, P. Walde, F. Gallou and B. H. Lipshutz, *Chem. Sci.*, 2021, **12**, 4237; (*b*) R. N. Butler, W. J. Cunningham and L. A. Burke, *J. Am. Chem. Soc.*, 2004, **126**, 11923.
10 N. Doshi, R. Fish, K. Padilla and S. Yadav, *J. Pharm. Sci.*, 2020, **109**, 2986.
11 A. Vallmitjana, A. Dvornikov, B. Torrado, D. M. Jameson, S. Ranjit and E. Gratton, *Methods Appl. Fluoresc.*, 2020, **8**, 035001.
12 (*a*) P. Shieh, V. T. Dien, B. J. Beahm, J. M. Castellano, T. Wyss-Coray and C. R. Bertozzi, *J. Am. Chem. Soc.*, 2015, **137**, 7145; (*b*) P. Shieh, M. Sloan Siegrist, A. J. Cullen and C. R. Bertozzi, *Proc. Natl. Acad. Sci. U. S. A.*, 2014, **111**, 5456.
13 W. Zhu, H. Qu, K. Xu, B. Jia, H. Li, Y. Du, G. Liu, H.-J. Wei and H.-Y. Zhao, *Anim. Cells Syst.*, 2017, **21**, 190.
14 H. Blom and J. Widengren, *Chem. Rev.*, 2017, **117**, 7377.
15 T. Nakabayashi and N. Ohta, *Anal. Sci.*, 2015, **31**, 275.

